IEEE Access
Multidisciplinary ⋮ Rapid Review ⋮ Open Access Journal

Received May 9, 2022, accepted June 10, 2022, date of publication June 16, 2022, date of current version June 23, 2022.

Digital Object Identifier 10.1109/ACCESS.2022.3183747

Event-Triggered Sliding Mode Control With Hysteresis for Motion Tracking of Piezoelectric Actuated Stage

NGUYEN NGOC SON, CAO VAN KIEN, AND TRAN MINH CHINH
Faculty of Electronics Technology, Industrial University of Ho Chi Minh City, Ho Chi Minh City 700000, Vietnam
Corresponding author: Nguyen Ngoc Son (nguyenngocson@iuh.edu.vn)

This work was supported by the Industrial University of Ho Chi Minh City (IUH) under Grant 79/HĐ-ĐHCN.

ABSTRACT In this study, an event-triggered sliding mode control with hysteresis is proposed for motion tracking of a piezoelectric actuator (PEA) in the presence of uncertainties, disturbances, and nonlinear hysteresis characteristics. First, the dynamic model with hysteresis characteristics of the piezoelectric actuator (PEA) is described by the Bouc-Wen model. Second, the design of an event-triggered sliding mode control (ETSMC) with hysteresis for the PEA system is discussed, and its stability is proved using Lyapunov's law. Finally, piezoelectric actuator PZS001 of THORLABS is used to validate the proposed controller. The simulation results demonstrated the effectiveness of the ETSMC approach.

INDEX TERMS Event-triggered control, sliding mode control (SMC), event-triggered sliding mode control, Bouc-Wen model, piezoelectric actuator (PEA).

I. INTRODUCTION

Piezoelectric actuators (PEA) produce a micro-displacement with high speed, force, and resolution. These actuators are widely used in various fields, including aerospace technology [1]–[4], microrobots [5]–[7], flexure-based XY platforms [8], and biological engineering [9]. However, the hysteresis nonlinearity and parametric uncertainties of piezoelectric actuators significantly affect motion-tracking precision and response time. To deal with the hysteresis effect, a mathematical model-based approach has been used to describe the hysteresis of PEA, such as the Bouc-Wen model [10], Prandtl-Ishlinskii model [11], Duhem model [12], and Preisach model [13].

To obtain a fast response time and high-quality control, sliding mode control (SMC) has been widely investigated to guarantee the stabilization of the hysteresis system in the presence of uncertainties and external disturbances [14]–[16]. However, a chattering phenomenon occurs, and the system trajectory slips in the vicinity of the sliding manifold when deploying SMC control to impact the accuracy and life of the system. To overcome these drawbacks, many different studies have been introduced to reduce the sliding band, and chattering phenomena, and improve accuracy. For example, neural network-based SMC control [17] was proposed to obtain robust adaptive precision motions of a piezoelectric-actuated system. Where, a singularity-free neural network was used to identify online and compensated. Feedback SMC control ensured stability. An extended state observer (ESO) applied to the RBFNN and SMC [18] was developed for motion tracking of the piezoelectric actuator. The ESO was used to cancel uncertainties and disturbances of the system and the RBFNN with SMC was deployed to improve accuracy. An adaptive neural network sliding mode control with hysteresis compensation [19] was proposed to improve the motion tracking of the piezoelectric actuator. An extended-state observer-based SMC [20] was developed to cancel the unmodelled dynamics and disturbances of the system. Sliding mode neural fuzzy control [21] was introduced to address the vibration of a double flexible beam system equipped with an AC servomotor and piezoelectric actuators. In which, a neural-fuzzy model was used to alleviate the chattering phenomenon.

In recent years, event-triggered control has received attention due to its advantages in terms of saving computational resources. Unlike classical time-driven control with sampled data, control tasks are not executed until an event-triggering strategy is satisfied. In which, an event-triggering strategy is designed to generate a triggering instant for sampling and updating the control signal for closed-loop system stability.

The associate editor coordinating the review of this manuscript and approving it for publication was Zheng Chen.

Therefore, event-triggered control has been widely applied in many types of nonlinear systems such as multiagent systems [22], [23], time-delay system [24], [25], fault-tolerant systems [26], [27], and nonlinear hysteresis systems [28]–[30]. Based on the advantages of event-triggered control, a combination of SMC and event-triggered control should be considered to reduce the sliding band and improve the control performance of the system [31]–[34].

In this paper, an event-triggered sliding mode control (ETSMC) with hysteresis is proposed for motion tracking of piezoelectric actuator (PEA). First, the hysteresis characteristics of the piezoelectric actuator (PEA) are described by the Bouc-Wen model. Second, the design of event-triggered sliding mode control for the PEA system is discussed and proved the stability. Finally, the Bouc-Wen parameters of piezoelectric actuator PZS001 of THORLABS which are identified using aDE-Jaya algorithms [10], are used to validate the proposed controller.

The rest of this paper is structured with the Section 2 presenting the dynamic model of the PEA system. Section 3 presents the proposed ETSMC control. Section 4 analyses and discusses the motion tracking control of the PEA system. Finally, Section 5 presents the conclusions.

II. DYNAMIC MODEL OF PIEZOELECTRIC ACTUATOR

The Bouc-Wen model was used to describe the hysteresis characteristics of the piezoelectric actuator (PEA), which is expressed as

$$M\ddot{y}(t) + B\dot{y}(t) + Ky(t) = K(Pu(t) - h(t)) \quad (1)$$

$$\dot{h}(t) = \alpha P\dot{u}(t) - \beta |\dot{u}(t)| h(t) - \gamma \dot{u}(t) |h(t)| \quad (2)$$

where u and y represent the input voltage and output displacement of the piezoelectric actuator respectively. Where *M, B, and K* are the equivalent mass, damping coefficient, and stiffness coefficient respectively. P represents the piezoelectric coefficient. h is a hysteresis term of the Bouc-Wen model and coefficients α, β, and γ influence the shape and magnitude of the hysteresis curve.

The parameters (M, B, K, P, α, β, and γ) of the PEA system can be identified by minimizing the objective function as follows

$$f(M, B, K, P, \alpha, \beta, \gamma) = \frac{1}{N}\sum_{i=1}^{N}\left(yr_i - yBW_i\right)^2 \quad (3)$$

where *yr* represents the displacement of the experimental PEA system, *yBW* represents the Bouc-Wen model output.

III. EVENT-TRIGGERED SLIDING MODE CONTROL

A. DESIGN OF SLIDING MODE CONTROL

From (1), we define $x_1 = y$, *and* the state-space of the PEA system is determined as,

$$\begin{cases} \dot{x}_1 = x_2 \\ \dot{x}_2 = -\frac{K}{M}x_1 - \frac{B}{M}x_2 + \frac{K}{M}(Pu - h) \end{cases} \quad (4)$$

where $f_1(x) = -\frac{K}{M}x_1 - \frac{B}{M}x_2$, $g_1(x) = \frac{K}{M}P$. We denote $f(x) = \begin{bmatrix} x_2 \\ f_1(x) \end{bmatrix}$. To design the ETSMC, the tracking error is defined as

$$\begin{cases} \tilde{x}_1 = x_1 - x_d \\ \tilde{x}_2 = x_2 - \dot{x}_d \end{cases} \quad (5)$$

where $x_d(t)$ and $x(t)$ represent the desired displacement and actual displacement of the PEA system, respectively. From (4), (5), and (6), we obtain

$$\begin{cases} \dot{\tilde{x}}_1 = \tilde{x}_2 \\ \dot{\tilde{x}}_2 = f_1(\tilde{x}) + g_1(x)u - \frac{K}{M}h - \ddot{x}_d - \frac{K}{M}x_d - \frac{B}{M}\dot{x}_d \end{cases} \quad (6)$$

We denote $f(\tilde{x}) = \begin{bmatrix} \tilde{x}_2 \\ f_1(\tilde{x}) \end{bmatrix} = \begin{bmatrix} \tilde{x}_2 \\ -\frac{K}{M}\tilde{x}_1 - \frac{B}{M}\tilde{x}_2 \end{bmatrix}$.

The following assumptions are considered as

Assumption 1: The desired displacement $x_d(t)$ is bounded and differentiable, and the second derivative of $x_d(t)$ exists, and is bounded.

Assumption 2: The function $f(.)$ is Lipschitz in a compact domain $D \in R^n$.

The sliding surface is defined as follows

$$s = c^T\tilde{x} \quad (7)$$

where, $c^T = \left[c_1^T\ 1\right]$ with $c_1 \in R^{n-1}$ and $\tilde{x} = \left[\tilde{x}_1^T\tilde{x}_2\right]^T$.

We design the control input as

$$u = -\frac{1}{g_1(x)}(c^T f(\tilde{x}) + K_s sign s - \frac{K}{M}h - \ddot{x}_d - \frac{K}{M}x_d - \frac{B}{M}\dot{x}_d) \quad (8)$$

where $K_s > 0$.

Theorem 1: Consider the PEA system (1) with the sliding surface (7), the tracking error $\tilde{x} = \left[\tilde{x}_1^T\tilde{x}_2\right]^T$ satisfies $\lim_{t\to\infty}\tilde{x} = 0$ if the control law is given by (8).

Proof: The Lyapunov function is selected $V = \frac{1}{2}s^2$. Differentiating V can be obtained as

$$\dot{V} = s\dot{s} \quad (9)$$

Taking the time derivative of (7) obtains

$$\begin{aligned} \dot{s} &= c_1^T\dot{\tilde{x}}_1 + \dot{\tilde{x}}_2 \\ &= c_1^T\tilde{x}_2 + \dot{x}_2 - \ddot{x}_d \\ &= c_1^T\tilde{x}_2 - \frac{K}{M}x_1 - \frac{B}{M}x_2 + g_1(x)u - \frac{K}{M}h - \ddot{x}_d \\ &= c_1^T\tilde{x}_2 - \frac{K}{M}\tilde{x}_1 - \frac{B}{M}\tilde{x}_2 - \frac{K}{M}x_d - \frac{B}{M}\dot{x}_d + g_1(x)u \\ &\quad - \frac{K}{M}h - \ddot{x}_d \\ &= c^T f(\tilde{x}) + g_1(x)u - \frac{K}{M}h - \frac{K}{M}x_d - \frac{B}{M}\dot{x}_d - \ddot{x}_d \end{aligned} \quad (10)$$

Substituting (10) into (9), we can obtain

$$\dot{V} = s(c^T f(\tilde{x}) + g_1(x)u - \frac{K}{M}h - \frac{K}{M}x_d - \frac{B}{M}\dot{x}_d - \ddot{x}_d) \quad (11)$$

Next, substituting (8) into (11) yields

$$\begin{aligned}\dot{V} &= s(c^T f(\tilde{x}) - (c^T f(\tilde{x}) + K_s signs - \frac{K}{M}h - \ddot{x}_d - \frac{K}{M}x_d \\ &\quad - \frac{B}{M}\dot{x}_d) - \frac{K}{M}h - \frac{K}{M}x_d - \frac{B}{M}\dot{x}_d - \ddot{x}_d) \\ &= s(-K_s signs) \le -K_s |s| \end{aligned} \tag{12}$$

Since $K_s > 0$, we deduce that $\dot{V} < 0$.

B. EVENT-TRIGGERED SLIDING MODE CONTROL

For the event-triggered mechanism, the corresponding control signal is given as

$$u(t) = u(t_i), \quad \forall t \in [t_i, t_{i+1}) \tag{13}$$

where $\{t_i\}_{i=1}^{\infty}$ and $t_0 = 0$ is defined as the event-trigger instants generated by the event-triggering strategy, and $T_i = t_{i+1} - t_i$ is the inter-event time.

Define the event-trigger error $e(t) = \tilde{x}(t_i) - \tilde{x}(t)$, where $t \in [t_i\ t_{i+1})$. The control signal can be written as

$$\begin{aligned}u(t) = -\frac{1}{g_1(x)}(c^T f(\tilde{x}(t_i)) + K_s signs(t_i) \\ - \frac{K}{M}h - \ddot{x}_d - \frac{K}{M}x_d - \frac{B}{M}\dot{x}_d)\end{aligned} \tag{14}$$

Theorem 2: Consider the nonlinear system in (1) and the control law in (14). Let $\mu > 0$ be given that

$$L \|c\| \|e(t)\| < \mu \tag{15}$$

For all time $t \ge 0$. The gain K_s is chosen as

$$K_s > \mu \tag{16}$$

Proof: The Lyapunov function is selected as $V = \frac{1}{2}s^2$. Differentiating V with $t \in [t_i t_{i+1})$ can be obtained as

$$\begin{aligned}\dot{V}(s) &= s\dot{s} \\ &= s(c^T f(\tilde{x}) + g_1(x)u - \frac{K}{M}h - \frac{K}{M}x_d - \frac{B}{M}\dot{x}_d - \ddot{x}_d)\end{aligned} \tag{17}$$

Substituting (14) into (17), we obtain

$$\begin{aligned}&\dot{V}(s(t)) \\ &= s(t)\left(c^T f(\tilde{x}(t)) - c^T f(\tilde{x}(t_i)) - K_s signs(t_i)\right) \\ &\le -s(t) K_s signs(t_i) + |s(t)| \left\| c^T f(\tilde{x}(t)) - c^T f(\tilde{x}(t_i)) \right\| \\ &\le -s(t) K_s signs(t_i) + |s(t)| \|c\| \|f(\tilde{x}(t)) - f(\tilde{x}(t_i))\| \\ &\le -s(t) K_s signs(t_i) + |s(t)| L \|c\| \|\tilde{x}(t) - \tilde{x}(t_i)\| \\ &= -s(t) K_s signs(t_i) + |s(t)| L \|c\| \|e(t)\|\end{aligned} \tag{18}$$

It is known that the sliding variable does not change until it reaches the sliding manifold, so it can be conducted that $signs(t_i) = signs(t)$. Substituting (15) into (18), we can obtain as

$$\begin{aligned}\dot{V}(s(t)) &\le -|s(t)| K_s + |s(t)| \mu \\ &= -|s(t)| (K_s - \mu) \\ &< -\rho |s(t)|\end{aligned} \tag{19}$$

where $\rho > 0$ such that $K_s > \mu$. From this $\dot{V}(s(t)) < 0$, the system trajectory can move toward the sliding manifold $s(t) = 0$ during the time interval $t \in [t_i t_{i+1})$. When $signs(t_i) \ne signs(t)$, $\dot{V}(s(t)) < 0$ cannot be guaranteed. However, from (15), we can see that the system trajectory can be maintained in the ultimate region, which can be calculated as

$$\begin{aligned}|s(t_i) - s(t)| &= \left| c^T \tilde{x}(t_i) - c^T \tilde{x}(t) \right| \\ &\le \|c\| \|e(t)\| < \frac{\mu}{L}\end{aligned} \tag{20}$$

Based on this, the maximum value of region Ω can be obtained by setting $s(t_i) = 0$ and the band is given as

$$\Omega = \left\{ \tilde{x} \in D : |s| = \left| c^T \tilde{x} \right| < \frac{\mu}{L} \right\}$$

It can be seen that the closed-loop system has finite-time convergence into a bounded set Ω. Thus, the proof is completed.

Remark 1: The value of μ determines the steady-state bound of trajectory tracking. So, μ is chosen for the next triggering instant to be larger than the sampling intervals of hardware.

C. EVENT-TRIGGERING RULE

The event-trigger rule must be designed by using condition (15) to ensure the system stability. To guarantee the condition (15) is always true for all times $t \ge 0$, the triggering mechanism is formulated as

$$t_{i+1} = inf(t > t_i : L \|c\| \|e(t)\| \ge \sigma\mu) \tag{21}$$

where $\sigma \in (0, 1)$.

Theorem 3: Consider the nonlinear system in (1) and the control law in (14). Let $\{t_i\}_{i=0}^{\infty}$ be a triggering sequence generated by the triggering rule (21). Then, the inter-event time $T_i = t_{i+1} - t_i$ is lower-bounded by a positive value and given as

$$T_i \ge \frac{1}{L} ln\left(1 + \sigma \frac{\mu}{\|c\| (\rho(\|\tilde{x}(t_i)\|) + K_s)}\right) \tag{22}$$

where,

$$\rho(\|\tilde{x}(t_i)\|) = (1 + \|c\|) L \|\tilde{x}(t_i)\|$$

Proof: The time required for event-trigger error $\|e\|$ to rise from zero to $\frac{\sigma\mu}{L\|c\|}$ should be lower bounded. From (6), the event-driven system is represented as

$$\dot{\tilde{x}} = f(\tilde{x}) + g_1 u - \frac{K}{M}h - \ddot{x}_d - \frac{K}{M}x_d - \frac{B}{M}\dot{x}_d \tag{23}$$

Consider $e(t)$ on interval $[t_i t_{i+1})$, we have

$$\begin{aligned}\frac{d}{dt}\|e(t)\| &\le \left\| \frac{d}{dt} e(t) \right\| = \left\| \frac{d}{dt} \tilde{x}(t) \right\| \\ &= \left\| f(\tilde{x}) + g_1 u - \frac{K}{M}h - \ddot{x}_d - \frac{K}{M}x_d - \frac{B}{M}\dot{x}_d \right\| \\ &= \left\| f(\tilde{x}) - (c^T f(\tilde{x}(t_i)) + K_s signs(t_i) - \frac{K}{M}h - \ddot{x}_d \right.\end{aligned}$$

TABLE 1. Identified PZS001 model paramerers.

Parameters	Value
M	0.0059
B	0.2336
K	58.8796
P	0.0184
α	0.5724
β	0.0087
γ	0.1137

$$-\frac{K}{M}x_d - \frac{B}{M}\dot{x}_d) - \frac{K}{M}h - \ddot{x}_d - \frac{K}{M}x_d - \frac{B}{M}\dot{x}_d\Big\| = \left\|f(\tilde{x}) - c^T f(\tilde{x}(t_i)) - K_s signs(t_i)\right\| \quad (24)$$

Substituting $e(t) = \tilde{x}(t_i) - \tilde{x}(t)$ into (24), we have

$$\begin{aligned}\frac{d}{dt}\|e(t)\| &\le L\|\tilde{x}(t)\| + \left\|c^T f(\tilde{x}(t_i))\right\| + K_s \\ &\le L(\|\tilde{x}(t_i)\| + \|e(t)\|) + L\|c\|\,\|\tilde{x}(t_i)\| + K_s \\ &= L\|e(t)\| + (1 + \|c\|)L\|\tilde{x}(t_i)\| + K_s \\ &= L\|e(t)\| + \rho(\|\tilde{x}(t_i)\|) + K_s \end{aligned} \quad (25)$$

Solving the differential inequality (25) with the initial condition $\|e(t_i)\| = 0$, we have

$$\|e(t)\| \le \frac{\rho(\|\tilde{x}(t_i)\|) + K_s}{L}(e^{L(t-t_i)} - 1) \quad (26)$$

At the instant of triggering t_{i+1}, $L\|c\|\,\|e(t_{i+1})\| = \sigma\mu$, so we write (26) as

$$\frac{\sigma\mu}{L\|c\|} = \|e(t_{i+1})\| \le \frac{\rho(\|\tilde{x}(t_i)\|) + K_s}{L}(e^{LT_i} - 1) \quad (27)$$

Rearranging (27) gives the expression (22) for inter-execution time. This shows that the inter-execution time will be lower bounded by some finite-positive quantity.

Remark 2: Theorem 3 ensures that $T_i > 0$ and will be lower bounded in domain Ω. So, the boundedness on T_i ensures robust trajectory tracking.

IV. RESULTS AND DISCUSSION

In this paper, the piezoelectric actuator PZS001 (PEA) of THORLABS is used to validate the proposed controller (thorlabs.com/thorproduct.cfm?partnumber=PZS001). The dynamic model of the PZS001 actuator is expressed as (1). The dynamic parameters (M, B, K, P, α, β, and γ) were identified by using aDE-Jaya algorithms [10] based on the input and output experimental PZS001 system, as shown in Table 1.

Design a sliding surface as $s = c^T\tilde{x} = [0.5\ 1]'\tilde{x}$. The ETSMC parameters are chosen as $K_s = 8$, $\sigma = 0.1$, $\mu = 0.1$, $L = 10$. To validate the performance of the ETSMC, the trajectory references are used including a case 1 – step response, and case 2 – sinusoidal signal.

The simulation results of case 1 are shown in Fig.1-2. Fig.1 shows the trajectory tracking and the control input.

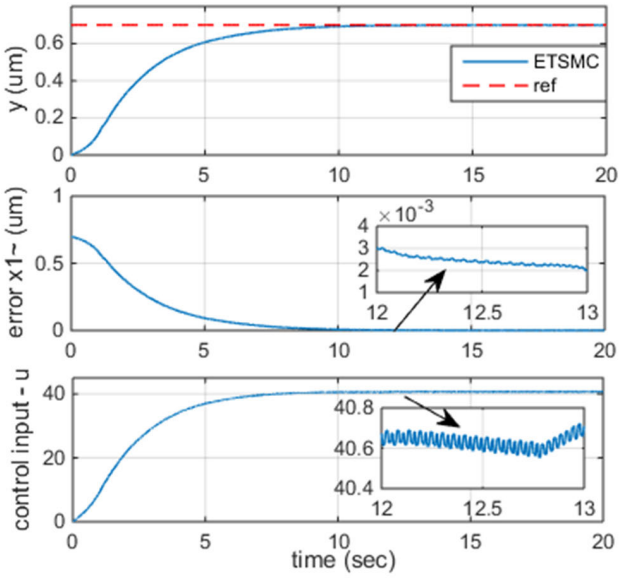

FIGURE 1. Time responses of state trajectory, error $\tilde{x}_1(t)$ and control input of ETSMC in case 1.

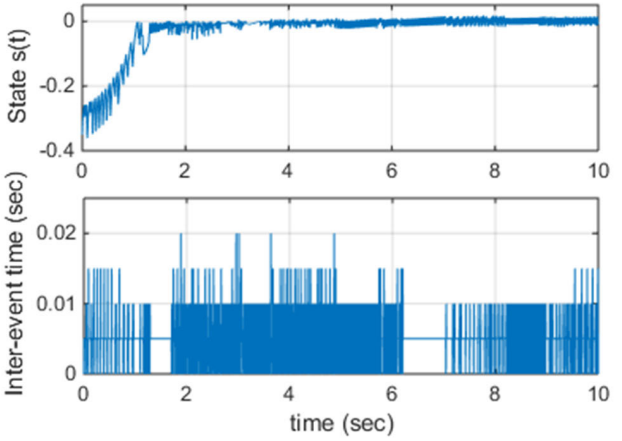

FIGURE 2. Time responses of sliding surface $s(t)$ and inter-event period of ETSMC in case 1.

We can see from Fig.1 that the PEA can track the desired trajectory in 9 (sec) and the tracking steady-state error are $|\tilde{x}_1| \le 3 \times 10^{-3}$. Fig.1 also shows that the control input remains constant until the event is triggered. Fig.2 shows the sliding variable state s(t) and the inter-event time. After a finite time, the trajectory reaches the sliding manifold and remains bounded around the region near zero. Fig.2 also shows that the lower bound of the inter-event time is 0.005 and the maximum is 0.02.

The simulation results for case 2 are shown in Fig.3-4. Fig.3 shows that PEA can track the desired trajectory in terms of the setting time of 7 (sec), tracking error of $|\tilde{x}_1| \le 0.005$. Fig.4 shows the trajectory reaches the sliding manifold and remains bounded around the region near zero. Fig.4 also

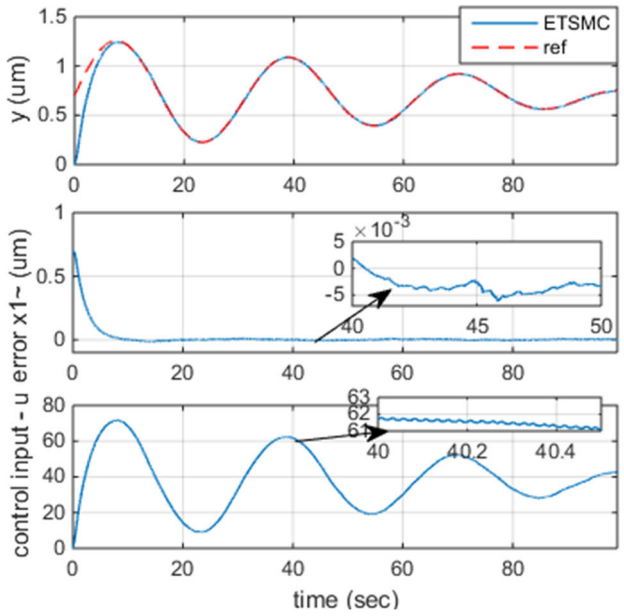

FIGURE 3. Time responses of state trajectory, error $\tilde{x}_1(t)$ and control input of ETSMC in case 2.

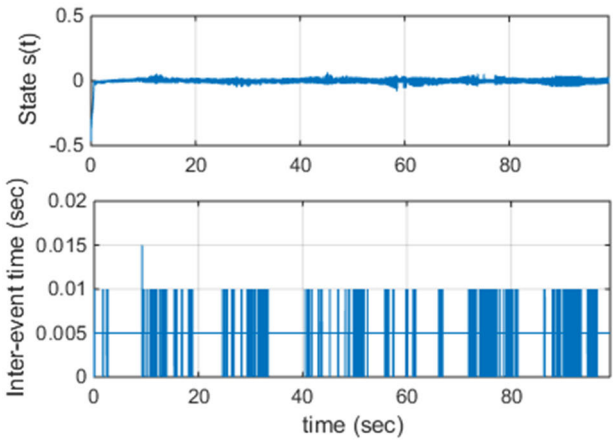

FIGURE 4. Time responses of sliding surface $s(t)$ and inter-event period of ETSMC in case 2.

shows the lower bound of the inter-event time is 0.005 and the maximum is 0.0015.

Based on the above results, we can see that all signals are bounded and the event-triggered sliding mode control can obtain tracking control accuracy.

V. CONCLUSION

This paper presents the event-triggered sliding mode control (ETSMC) with hysteresis for motion tracking of the piezoelectric actuated stage. The event-triggering strategy was discussed and proven to guarantee asymptotic stability. The simulation results show that motion tracking can achieve accuracy, and all closed-loop signals are bounded. However, the ETSMC controller still has some drawbacks. such as a large setting time, not yet self-adapting, and the existing chattering phenomenon. Future work will focus on a hybrid adaptive event-triggered sliding mode control-based neural networks and hysteresis compensation to further improve the tracking accuracy.

REFERENCES

[1] E. Zhang, Y. Hu, H. Bao, J. Li, J. Ma, and J. Wen, "A linear inertial piezoelectric actuator using a single bimorph vibrator," *Smart Mater. Struct.*, vol. 28, no. 11, Nov. 2019, Art. no. 115020.

[2] H. Elahi, "The investigation on structural health monitoring of aerospace structures via piezoelectric aeroelastic energy harvesting," *Microsyst. Technol.*, vol. 27, no. 7, pp. 2605–2613, Jul. 2021.

[3] S. Zhang, Y. Liu, J. Deng, X. Tian, and X. Gao, "Development of a two-DOF inertial rotary motor using a piezoelectric actuator constructed on four bimorphs," *Mech. Syst. Signal Process.*, vol. 149, Feb. 2021, Art. no. 107213.

[4] Y. Hu, R. Wang, J. Wen, and J.-Q. Liu, "A low-frequency structure-control-type inertial actuator using miniaturized bimorph piezoelectric vibrators," *IEEE Trans. Ind. Electron.*, vol. 66, no. 8, pp. 6179–6188, Aug. 2019.

[5] T. Abondance, K. Jayaram, N. T. Jafferis, J. Shum, and R. J. Wood, "Piezoelectric grippers for mobile micromanipulation," *IEEE Robot. Autom. Lett.*, vol. 5, no. 3, pp. 4407–4414, Jul. 2020.

[6] X. Gao, J. Deng, S. Zhang, J. Li, and Y. Liu, "A compact 2-DOF micro/nano manipulator using single miniature piezoelectric tube actuator," *IEEE Trans. Ind. Electron.*, vol. 69, no. 4, pp. 3928–3937, Apr. 2022.

[7] J. Li, Y. Liu, J. Deng, S. Zhang, and W. Chen, "Development of a linear piezoelectric microactuator inspired by the hollowing art," *IEEE Trans. Ind. Electron.*, vol. 69, no. 10, pp. 10407–10416, Oct. 2022.

[8] X. Gao, Y. Liu, S. Zhang, J. Deng, and J. Liu, "Development of a novel flexure-based XY platform using single bending hybrid piezoelectric actuator," *IEEE/ASME Trans. Mechatronics*, early access, Feb. 24, 2022, doi: 10.1109/TMECH.2022.3150399.

[9] J. Deng, W. Chen, K. Li, L. Wang, and Y. Liu, "A sandwich piezoelectric actuator with long stroke and nanometer resolution by the hybrid of two actuation modes," *Sens. Actuators A, Phys.*, vol. 296, pp. 121–131, Sep. 2019.

[10] N. N. Son, C. Van Kien, and H. P. H. Anh, "Parameters identification of Bouc–Wen hysteresis model for piezoelectric actuators using hybrid adaptive differential evolution and Jaya algorithm," *Eng. Appl. Artif. Intell.*, vol. 87, Jan. 2020, Art. no. 103317, doi: 10.1016/j.engappai.2019.103317.

[11] Y. Feng and Y. Li, "System identification of micro piezoelectric actuators via rate-dependent prandtl-ishlinskii hysteresis model based on a modified PSO algorithm," *IEEE Trans. Nanotechnol.*, vol. 20, pp. 205–214, 2021.

[12] R. Dong, Y. Tan, and Y. Xie, "Identification of micropositioning stage with piezoelectric actuators," *Mech. Syst. Signal Process.*, vol. 75, pp. 618–630, Jun. 2016.

[13] Z. Li, J. Shan, and U. Gabbert, "Inverse compensator for a simplified discrete Preisach model using model-order reduction approach," *IEEE Trans. Ind. Electron.*, vol. 66, no. 8, pp. 6170–6178, Aug. 2019.

[14] S. Kang, H. Wu, X. Yang, Y. Li, J. Yao, B. Chen, and H. Lu, "Discrete-time predictive sliding mode control for a constrained parallel micropositioning piezostage," *IEEE Trans. Syst., Man, Cybern., Syst.*, vol. 52, no. 5, pp. 3025–3036, May 2022.

[15] Y. Zhang and P. Yan, "Adaptive observer-based integral sliding mode control of a piezoelectric nano-manipulator," *IET Control Theory Appl.*, vol. 13, no. 14, pp. 2173–2180, Sep. 2019.

[16] R. Xu, X. Zhang, H. Guo, and M. Zhou, "Sliding mode tracking control with perturbation estimation for hysteresis nonlinearity of piezo-actuated stages," *IEEE Access*, vol. 6, pp. 30617–30629, 2018.

[17] J. Ling, Z. Feng, D. Zheng, J. Yang, H. Yu, and X. Xiao, "Robust adaptive motion tracking of piezoelectric actuated stages using online neural-network-based sliding mode control," *Mech. Syst. Signal Process.*, vol. 150, Mar. 2021, Art. no. 107235.

[18] J. Y. Lau, W. Liang, and K. K. Tan, "Motion control for piezoelectric-actuator-based surgical device using neural network and extended state observer," *IEEE Trans. Ind. Electron.*, vol. 67, no. 1, pp. 402–412, Jan. 2020.

[19] N. N. Son, C. Van Kien, and H. P. H. Anh, "Adaptive sliding mode control with hysteresis compensation-based neuroevolution for motion tracking of piezoelectric actuator," *Appl. Soft Comput.*, vol. 115, Jan. 2022, Art. no. 108257.

[20] S. Yu, Y. Feng, and X. Yang, "Extended state observer-based fractional order sliding-mode control of piezoelectric actuators," *Proc. Inst. Mech. Eng. I, J. Syst. Control Eng.*, vol. 235, no. 1, pp. 39–51, 2021.
[21] Z. C. Qiu and S. W. Chen, "Vibration control of a translational coupled double flexible beam system using sliding mode neural network fuzzy control," *Trans. Inst. Meas. Control*, vol. 44, no. 11, pp. 2264–2288, 2022.
[22] Z.-G. Wu, Y. Xu, Y.-J. Pan, H. Su, and Y. Tang, "Event-triggered control for consensus problem in multi-agent systems with quantized relative state measurements and external disturbance," *IEEE Trans. Circuits Syst. I, Reg. Papers*, vol. 65, no. 7, pp. 2232–2242, Jul. 2018.
[23] X. Li, Y. Tang, and H. R. Karimi, "Consensus of multi-agent systems via fully distributed event-triggered control," *Automatica*, vol. 116, Jun. 2020, Art. no. 108898.
[24] J. Sun, J. Yang, and Z. Zeng, "Predictor-based periodic event-triggered control for nonlinear uncertain systems with input delay," *Automatica*, vol. 136, Feb. 2022, Art. no. 110055.
[25] Q. Li, B. Shen, Z. Wang, T. Huang, and J. Luo, "Synchronization control for a class of discrete time-delay complex dynamical networks: A dynamic event-triggered approach," *IEEE Trans. Cybern.*, vol. 49, no. 5, pp. 1979–1986, May 2019.
[26] X. Zhang, J. Tan, J. Wu, and W. Chen, "Event-triggered-based fixed-time adaptive neural fault-tolerant control for stochastic nonlinear systems under actuator and sensor faults," *Nonlinear Dyn.*, vol. 108, no. 3, pp. 2279–2296, 2022.
[27] Q.-Y. Fan and G.-H. Yang, "Event-based fuzzy adaptive fault-tolerant control for a class of nonlinear systems," *IEEE Trans. Fuzzy Syst.*, vol. 26, no. 5, pp. 2686–2698, Oct. 2018.
[28] J. Wang, H. Zhang, K. Ma, Z. Liu, and C. L. P. Chen, "Neural adaptive self-triggered control for uncertain nonlinear systems with input hysteresis," *IEEE Trans. Neural Netw. Learn. Syst.*, early access, May 10, 2021, doi: 10.1109/TNNLS.2021.3072784.
[29] J. Wang, Z. Liu, Y. Zhang, and C. L. P. Chen, "Neural adaptive event-triggered control for nonlinear uncertain stochastic systems with unknown hysteresis," *IEEE Trans. Neural Netw. Learn. Syst.*, vol. 30, no. 11, pp. 3300–3312, Nov. 2019.
[30] L. Cao, H. Ren, H. Li, and R. Lu, "Event-triggered output-feedback control for large-scale systems with unknown hysteresis," *IEEE Trans. Cybern.*, vol. 51, no. 11, pp. 5236–5247, Nov. 2021.
[31] A. K. Behera, B. Bandyopadhyay, and X. Yu, "Periodic event-triggered sliding mode control," *Automatica*, vol. 96, pp. 61–72, Oct. 2018.
[32] X. Su, X. Liu, P. Shi, and Y.-D. Song, "Sliding mode control of hybrid switched systems via an event-triggered mechanism," *Automatica*, vol. 90, pp. 294–303, Apr. 2018.
[33] B.-C. Zheng, X. Yu, and Y. Xue, "Quantized feedback sliding-mode control: An event-triggered approach," *Automatica*, vol. 91, pp. 126–135, May 2018.
[34] A. Behera and B. Bandyopadhyay, "Robust sliding mode control: An event-triggering approach," *IEEE Trans. Circuits Syst. II, Exp. Briefs*, vol. 64, no. 2, pp. 146–150, Feb. 2017.

NGUYEN NGOC SON received the M.Sc. and Ph.D. degrees from the Faculty of Electrical and Electronics Engineering (FEEE), Ho Chi Minh City University of Technology, in 2012 and 2017, respectively. He is currently a Lecturer with the Faculty of Electronics Technology, Industrial University of Ho Chi Minh City, Vietnam. His current research interests include artificial intelligence, robotics, identification, intelligent control, and the Internet of Things.

CAO VAN KIEN received the M.Sc. and Ph.D. degrees from the Faculty of Electrical and Electronics Engineering (FEEE), HCM City University of Technology, in 2016 and 2022, respectively. He is currently a Lecturer with the Faculty of Electronics Technology, Industrial University of Ho Chi Minh City. His current research interests include intelligent control, robotics, and soft computing.

TRAN MINH CHINH received the Ph.D. degree from Tambov State Technical University, Russia, in 2016. He is currently a Lecturer with the Faculty of Electronics Technology, Industrial University of Ho Chi Minh City. His current research interests include advanced control theory, robotics, and soft computing.